Development of a Dynamic PV/T-Driven Combined Cooling, Heating and Power System Model for Use in the Canadian Residential Sector

Cem Kalkan[1], Jean Duquette[1], Fidel Khouli[1], Amer Keblawi[1], Mehmet Akif Ezan[2]
[1] Carleton University, Ottawa, Canada
[2] Dokuz Eylul University, Izmir, Turkey

Abstract

Photovoltaic-Thermal (PV/T)-driven combined cooling, heating, and power (CCHP) systems have been identified as a technically feasible low-carbon alternative for providing critical building energy services. However, few numerical modelling studies accurately predict the dynamic response exhibited by these systems. In this study, transient numerical models (implemented in the MATLAB® simulation environment) representing a single-effect LiBr-H_2O absorption chiller and a PV/T collector array are developed and integrated into a larger PV/T-driven CCHP system model in TRNSYS 18. Further to model validation, the system is shown to be capable of supplying 27.10% of the daily space heating load on a peak winter day. This model will be used as a basis for further system optimization.

Introduction

In 2015, while participating in the United Nations Climate Change Conference in Paris, Canada committed to reducing greenhouse gas emissions by 30% by 2030. Recently, the Canadian federal government has increased this emissions reduction target to 40-45% and promised to achieve net-zero emissions by 2050 (Langlois-Bertrand et al., 2021). Although a newly introduced carbon pricing policy, which is set to increase the price of carbon by $170 per tonne by 2030, is expected to accelerate Canada's path to decarbonisation (Sawyer et al., 2021), significant efforts are also needed with regards to emissions reductions in Canada's major economic sectors such as the buildings sector. Buildings alone account for approximately 17% of Canada's total GHG emissions, with residential buildings making up roughly 60% of this total (House of Commons, 2018). Since burning fossil fuels for space heating and electricity production accounts for the greatest share of these emissions, there is a tremendous opportunity to lower emissions in the buildings sector by introducing renewably sourced fuels and sustainable energy conversion systems to provide cooling, heating, and power to buildings. Photovoltaic/Thermal (PV/T)-driven combined cooling, heating, and power (CCHP) systems are well suited for this purpose as they are currently widely used as an effective means of providing low-carbon energy for a number of applications (Youseffi et al., 2017; Kutlu et al., 2020).

PV/T-driven CCHP systems are a promising alternative which can be used to fulfil the heating, cooling and power requirements of a building. The potential for these systems to drastically decrease greenhouse gas emissions has helped them gain significant attention from the research community (Wang et al., 2010). The basic components of a PV/T-driven CCHP system include PV/T collectors, storage tank(s), a cooling device, and a heat rejection device. The system operates by harvesting heat from solar energy via the PV/T collectors. This harvested energy is used to drive the cooling device which extracts heat from the cooling medium that is stored in the cold storage tank. Any unused heat is stored in the hot storage tank. The domestic hot water (DHW) and space heating loads are supplied by the hot storage tank, whereas the cooling load is supplied from the cold storage tank. To operate the cooling device, a heat rejection device is required to dump the generated heat to the ambient. While supplying thermal energy to meet heating and cooling loads, PV/T collectors simultaneously generate electricity that is used to meet the building's electrical load.

Designers must carefully select the main components of PV/T-driven CCHP systems as many alternatives are possible. For example, instead of PV/T collectors, heat and electricity can be generated by solar thermal collectors and photovoltaic (PV) collectors separately. However, this alternative requires more installation space. Similarly, the cooling device can be thermally driven or electrically driven. Although electrically driven cooling devices are more common, thermally driven cooling devices can be integrated into the system in a cost-effective way (Zeyghami et al., 2015). Absorption chillers are more advantageous than other thermally driven cooling devices because this technology is reliable, mature, and energy-efficient (Shirazi et al., 2018).

Additionally, system components can be connected in a variety of configurations. Numerical methods enable researchers to investigate different system configuration alternatives in a short period of time without needing a physical experimental setup. However, care must be taken

to ensure that the system component models are fully validated. The system components can be modeled using either physics-based, data-based, or hybrid numerical methods. Within these categories, it is possible to use quasi-steady-state (QSS) numerical models, which ignore the thermal inertia of the component, or transient numerical models, which take thermal inertia into account.

Literature Review

There are a limited number of numerical studies focused on PV/T-driven CCHP systems in the literature that make use of an absorption chiller as the cooling device. For example, Herrando et al. (2019) numerically compared the performance of a PV/T-driven CCHP system with a standalone PV system for electricity provision, and evacuated tube collectors (ETC) for heating and cooling provision. In addition to PV/T collectors, their proposed system included a sensible hot storage tank and an absorption chiller. The model utilized an efficiency correlation-based model for the PV/T and evacuated tube collectors, a 1D model for the sensible energy storage tank, and a performance correlation-based model for the absorption chiller. The demand profiles of a building located at the University Campus of Bari, Italy, were used to develop scenarios in the comparison study. Their results showed that the system provided 20.9% and 55.1% of the heating and cooling demand, respectively. The authors of the paper concluded that PV/T-driven CCHP systems can play an important role in decarbonizing urban areas. In a separate study, Calise et al. (2012) investigated the performance of a PV/T-driven CCHP system consisting of PV/T collectors, a single-effect LiBr-H_2O absorption chiller, two hot storage tanks, a cold storage tank, a cooling tower, and an auxiliary heater. A zero-dimensional system model was developed in TRNSYS using the component library to model the system components and their operation. A case study of a university building located in Italy was considered to analyze the system performance from a technical and economic standpoint. Moreover, a parametric study was conducted to assess the impacts of varying a number of parameters on system performance. Results showed that from a cost-effectiveness standpoint, the best performance was achieved at values of 1200 m^2, 80 kg/h m^2, 80°C, and 10 L/m^2 for the PV/T collector area, flow rate per PV/T collector area, PV/T collector fluid setpoint temperature, and volume of hot storage tank per PV/T collector area, respectively.

Even though these recent research efforts have demonstrated that PV/T-driven CCHP systems hold considerable promise regarding decreasing building-based GHG emissions, the vast majority of studies in the literature are focused on systems consisting of stand-alone evacuated tube or flat plate collectors for generating heating and cooling services. For example, Fong and Lee (2015) investigated the performance of a solar heating and cooling system located in a low-rise residential building located in Hong Kong that consists of evacuated tube collectors, an auxiliary heater, a hot storage tank, an absorption chiller, and a cooling tower. They used an efficiency correlation-based model for the ETC array, a 1D model for the sensible energy storage tank and a performance correlation-based model for the absorption chiller. Two separate design alternatives (*i.e.* direct heat supply and indirect heat supply via a separate array of ETC collectors) were compared to supply the building's heating and cooling needs. The yearly performance of the design alternatives was compared with the conventional heating and cooling system under two different load scenarios using variable chilled water flow and on-off controllers. Results showed that the direct heat supply alternative provided energy savings of 17.7% and 18% in on-off and variable chilled water flow modes, respectively, whereas the indirect heat supply system achieved energy savings of 23% and 29.2%. In a similar work, Martinez et al. (2016) carried out simulations to assess the performance of a solar collector driven heating and cooling system which comprised an array of flat plate collectors, a hot storage tank, a cold storage tank, a cooling tower, a single-effect LiBr-H_2O absorption chiller, a back-up vapor compression heat pump, and a heat exchanger bank. The system model was built in the TRNSYS environment which uses a correlation-based model for the absorption chiller, a 1D model for the storage tank, and an efficiency correlation-based collector model. A temperature control algorithm that aims to keep the conditioned space at a set temperature was used in the system simulation. The system model was validated using an experimental setup located in Spain and the validated system model was used to simulate the performance of the system with and without the backup vapour compression heat pump under the summer working conditions of four different locations (*i.e.* Barcelona, Madrid, Bilbao, and Sevilla). Results revealed that in the first operation mode (*i.e.* cooling provided without the backup vapour-compression heat pump), the system maintained the setpoint temperature for 60.8% to 78.3% of the operation period. In the other operation mode (*i.e.* cooling provided with the backup vapour-compression heat pump), the absorption chiller provided 52.8% to 75.3% of the cooling demand to maintain the setpoint temperature.

PV/T-driven CCHP systems require complex topologies as they typically operate in various climates and changing environmental conditions. To operate optimally under these conditions, adequate system control strategies are required. Most control strategies for solar driven heating and cooling systems in the literature are tested using component models and algorithms available in the TRNSYS environment (Shirazi et al., 2018). Although several of the models from the TRNSYS component library are suitable for this purpose, some such as the absorption chiller model are largely inadequate, since this model uses performance data based correlations to simulate operation. Although the use of these correlations is advantageous due to fast associated simulation times, it is potentially problematic since the

thermal mass of the components is not considered. As a result, the TRNSYS absorption chiller model cannot provide accurate time-dependent information on the thermal behaviour of absorption chillers, and it is not suitable for dynamic system simulation (Kohlenbach and Ziegler, 2008; Bowie, 2006). Transient absorption chiller models should be used instead to model the effects occurring from the frequent changes in system operating conditions. Similarly, built-in models for PV/T collectors in TRNSYS do not consider the thermal inertia and dimensional effects of the collector layers. These simplifying assumptions affect the accuracy of the collector outputs (Tagliafico et al., 2014). Therefore, TRNSYS models cannot provide accurate information about the dynamic response of the collector, especially when there are dynamic changes in the operating conditions. These dynamic changes are frequent in the operation of a PV/T-driven CCHP system since PV/T collectors operate in conjunction with other system components. Improving the accuracy of the component models in the PV/T-driven CCHP system will in turn improve the quality of the strategies that are proposed to operate and control the system.

To address the research gap mentioned above, the current study has the following three objectives:

- Develop and verify/validate transient numerical models representing a single-effect LiBr-H_2O absorption chiller and a PV/T collector array in MATLAB®.
- Integrate these models in the TRNSYS 18 environment alongside other standard TRNSYS 18 component models to create a high-accuracy PV/T-driven CCHP system model that can be used as a basis for further system design optimization.
- Assess the system's heating performance for a typical day during the winter season.

Methods

A PV/T-driven CCHP system model is developed in the TRNSYS 18 environment using a multi-unit residential building located in Ottawa, Canada as the case study. The system layout is shown in Figure 1. The main components of the system are an array of PV/T collectors, a hot water storage tank, a LiBr-H_2O absorption chiller, an auxiliary heater, a heat exchanger, a cooling tower, and six pumps at different locations of the system.

Along with the built-in TRNSYS 18 component models, the system model includes the following two external models that are developed in MATLAB®: an absorption chiller model and a PV/T collector array model. To model the absorption chiller operation, a transient lumped parameter physics-based model, which assumes each component of the absorption chiller (*i.e.*, the generator, condenser, absorber, and evaporator) employs a unique pressure, temperature, and concentration. A number of mass and energy balance equations are solved to model the operation of each main component of the absorption chiller. The details of the equation system for the absorption chiller model can be found in Ochoa et al. (2016). The defined system of equations is discretized using the finite difference method with an explicit scheme. The numerical solution process is initially implemented in the MATLAB® environment. To solve the proposed system of equations, thermodynamic properties of various state points of the components, a specific solution order for the equations, and coupling between the equations are required. Details of the property calculations, tabulated data, and solution method utilized can be found in Ochoa et al. (2016). To model the PV/T collector operation, a 2D transient discretized physics-based model is used. The PV/T model considered in the study is composed of a glass cover, an air gap, PV cells, an absorber plate, box-shaped flow channels, and an insulation layer. The dimensions and thermophysical properties of the layers are adapted from the study of Chow et al. (2006). The energy balance equation is solved for each layer of the PV/T collector. To include the temporal variations of the PV/T collector, each layer is discretized in the flow direction. Figure 2. illustrates the layers of the PV/T collector and the discretization in the flow direction.

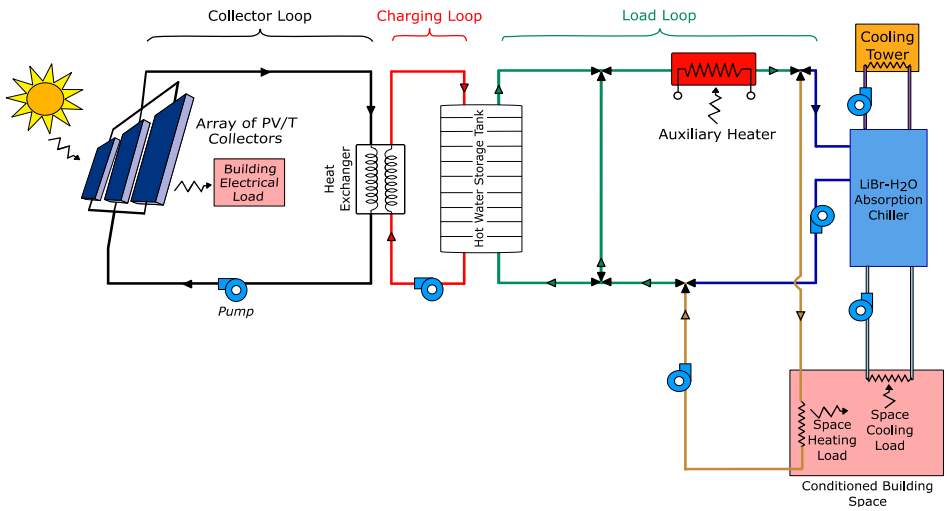

Figure 1. Layout of PV/T driven CCHP system model in TRNSYS 18. Transient PV/T collector array and absorption chiller models are developed in MATLAB® and integrated into the TRNSYS 18 environment

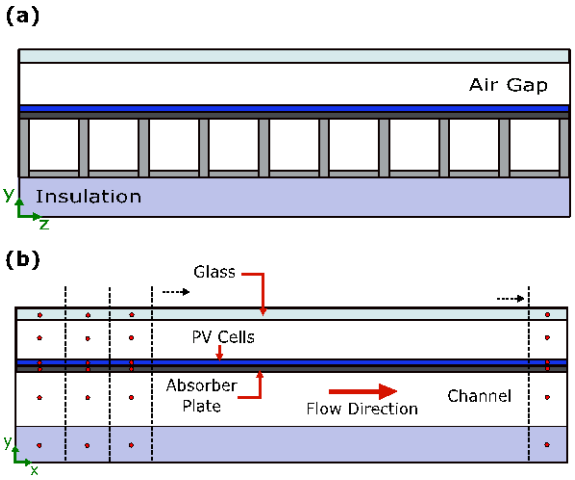

Figure 2. Layers of the PV/T collector and computational domains along the flow direction

The energy balance equation for the glass layer is given by the following equation:

$$\begin{aligned}\frac{m_g c_{p,g}\partial T_g}{\partial t} = \frac{k_g A_c \partial T_g}{\partial x} + I_{solar}\alpha_g A_s \\ +h_\infty A_s(T_\infty - T_g) + h_{rad}A_s(\mathrm{T_{sky}} - \mathrm{T_g}) \\ +h_{conv,in}\,A_s\left(T_{ag} - T_g\right) \\ +h_{rad,in}A_s\left(T_{PV} - T_g\right),\end{aligned} \quad (1)$$

where the term on the left-hand side of the equation represents the rate of change of thermal energy. The terms on the right-hand side (from left to right) represent the conductive heat transfer rate in the glass layer, the absorbed portion of the incoming solar irradiance, the convective heat loss to the ambient, the radiative heat loss to the ambient, the convective heat transfer to the air gap, and the radiative heat transfer to the PV layer. The convective heat transfer coefficient to the ambient (h_∞) is expressed as (Duffie et al., 2020)

$$h_\infty = 3.9\, v_{wind} + 5.62, \quad (2)$$

where v_{wind} represents the wind speed. The radiative heat transfer coefficient (h_{rad}) to the ambient is expressed as (Duffie et al., 2020)

$$h_{rad} = \varepsilon_g \sigma\left(T_{sky} + T_{sur}\right)\left(T_{sky}^2 + T_{sur}^2\right), \quad (3)$$

where the sky temperature is given by (Swinbank, 1963)

$$T_{sky} = 0.552 T_\infty^{1.5}\,. \quad (4)$$

The radiative heat transfer coefficient to the PV layer is expressed as follows (Duffie et al., 2020):

$$h_{rad,in} = \frac{\sigma\left(T_{PV} + T_g\right)\left(T_{PV}^2 + T_g^2\right)}{\frac{1}{\varepsilon_g} + \frac{1}{\varepsilon_{PV}}}. \quad (5)$$

The convective heat transfer coefficient to the air gap is expressed as

$$h_{conv,in} = \frac{Nu\, k_{ag}}{t_{ag}}, \quad (6)$$

where Nu is the Nusselt number given by (Duffie et al., 2020)

$$\begin{aligned}Nu = 1 + 1.44\left[1 - \frac{1708(\sin 1.8\,\theta)}{Ra}\right] \\ \left[1 - \frac{1708}{Ra\cos\theta}\right]^+ + \left[\left(\frac{Ra\cos\theta}{5380}\right)^{\frac{1}{3}} - 1\right]^+.\end{aligned} \quad (7)$$

The parameters θ and Ra in Equation 7 represent the collector tilt angle, and Rayleigh number, respectively. The terms bracketed by $[]^+$ are to be taken as zero if they are negative.

The air gap energy balance is expressed as:

$$\begin{aligned}\frac{m_{ag}c_{p,ag}\,\partial T_{ag}}{\partial t} = \frac{k_{ag}A_{ag}\partial T_{ag}}{\partial x} + \\ h_{conv,in}A_s\left(T_g - T_{ag}\right) - h_{conv,in}A_s\left(T_{PV} - T_{ag}\right),\end{aligned} \quad (8)$$

where the left-hand side term represents the heat storage rate of the air gap. The terms on the right-hand side (from left to right) represent heat transfer by conduction along the flow direction, the heat transfer by convection to the glass layer, and to the PV layer.

The PV layer energy balance is expressed as:

$$\begin{aligned}\frac{m_{PV}c_{p,PV}\partial T_{PV}}{\partial t} = k_{PV}\,A_{PV}\frac{\partial T_{PV}}{\partial x} + I_{solar}\tau_g\alpha_{PV}A_s \\ -\dot{E}_{PV} + h_{rad,in}A_s\left(T_g - T_{PV}\right) \\ +h_{conv,in}A_s\left(T_{ag} - T_{PV}\right) \\ +k_{har,PV-abs}\,A_s\frac{(T_{abs} - T_{PV})}{\Delta y_{PV-abs}},\end{aligned} \quad (9)$$

where the term on the left-hand side represents the rate of change of thermal energy of the PV layer, and the terms on the right-hand side (from left to right) represent the heat transfer by conduction along the flow direction of the heat transfer fluid, the rate of energy transmitted through the glass layer, the generated electricity in the PV cells, the heat transfer by radiation between the glass and PV layer, the heat transfer by conduction between the air gap and PV layer, and the heat transfer by conduction between the PV and absorber layer. The $k_{har,PV-abs}$ term in Equation (9) is the harmonic mean of the thermal conductivity of the PV cell and absorber (Patankar, 2018). The generated electricity from the PV cells ($\dot{E}_{PV}$) is calculated by the following equation:

$$\dot{E}_{PV} = \eta_{PV} I_{solar}\tau_g\alpha_{PV}A_{s,cell}, \quad (10)$$

where the electrical conversion efficiency of the PV cell (η_{PV}) is given by

$$\eta_{PV} = \eta_{Ref}\left(1 - \beta_{PV}\left(T_{PV} - T_{Ref}\right)\right). \quad (11)$$

In the current study, a polycrystalline silicon type PV cell with a nominal electrical efficiency of η_{Ref}= 0.145 and a temperature coefficient of β_{PV}= 0.005 1/K is used (Chow et al., 2006). T_{Ref} in Equation (11) represents the reference temperature and is equal to 298 K.

The absorber layer energy balance is expressed as:

$$\begin{aligned} m_{abs}c_{p,abs}\frac{\partial T_{abs}}{\partial t} &= k_{abs}A_{abs}\frac{\partial T_{abs}}{\partial x} \\ &+h_{HTF}A_{s,HTF}\left(T_f - T_{abs}\right) \\ &+\frac{k_{har,PV-abs}A_s(T_{PV} - T_{abs})}{\Delta y_{PV-abs}} \\ &+\frac{k_{har,abs-fin}2A_{s,fin}\left(T_{fin} - T_{abs}\right)}{\Delta y_{abs-fin}}, \end{aligned} \quad (12)$$

where the terms on the right-hand side (from left to right) represent the heat transfer by conduction along the flow direction in the absorber plate, the heat transfer by convection in the heat transfer fluid (HTF), the heat transfer by conduction between the absorber plate and the PV cells, and the heat transfer conduction between the side fins of the flow channel and the absorber plate. During normal operation, the heat transfer coefficient in the flow channel (h_{HTF}) can be calculated by the following Nusselt correlation (Duffie et al., 2020):

$$Nu = 5.4 + \frac{0.00021\left(\frac{Re\mathrm{PrD_h}}{L}\right)^{2.24}}{1 + 0.00060\left(\frac{Re\mathrm{PrD_h}}{L}\right)^{1.77}}, \quad (13)$$

where Re, Pr, and D_h represent the Reynolds number, Prandtl number and hydraulic diameter, respectively. Equations (14) and (15) presented below are solved for the side fins of the flow channel and bottom fin of the flow channel, respectively.

$$\begin{aligned} m_{fin}c_{p,fin}\frac{\partial T_{fin}}{\partial t} &= k_{fin}A_{fin}\frac{\partial T_{fin}}{\partial x} \\ &+h_{HTF}A_{l,fin}\left(T_f - T_{fin}\right) \\ &+\frac{k_{har,fin-bfin}\ A_{s,fin}\left(T_{bfin} - T_{fin}\right)}{\Delta y_{fin-bfin}} \\ &+k_{har,abs-fin}\ A_{s,fin}\frac{\left(T_{fin} - T_{abs}\right)}{\Delta y_{abs-fin}} \end{aligned} \quad (14)$$

$$\begin{aligned} m_{bfin}\ c_{p,bfin}\frac{\partial T_{bfin}}{\partial t} &= k_{bfin}\ A_{bfin}\ \frac{\partial T_{bfin}}{\partial x} \\ &+\frac{k_{har,fin-bfin}\ 2A_{s,fin}\ \left(T_{fin} - T_{bfin}\right)}{\Delta y_{fin-bfin}} \\ &+h_{HTF}\ A_{s,HTF}\ \left(T_f - T_{bfin}\right) \\ &+\frac{k_{har,bfin-ins}\ A_{ins}\ \left(T_{ins} - T_{bfin}\right)}{\Delta y_{bfin-ins}}. \end{aligned} \quad (15)$$

The energy balance describing the HTF inside the flow channels is expressed as:

$$\begin{aligned} m_f\ c_{p,f}\ \frac{\partial T_f}{\partial t} &= k_f\ A_{c,HTF}\ \frac{\partial T_f}{\partial x} \\ &+\dot{m}c_{p,f}\left(T_{f,inlet} - T_{f,outlet}\right) \\ &+h_{HTF}A_{s,HTF}\left(T_{abs} - T_f\right) \\ &+h_{HTF}2A_{l,fin}\left(T_{fin} - T_f\right) \\ &+h_{HTF}A_{s,HTF}\left(T_{bfin} - T_f\right), \end{aligned} \quad (16)$$

where the terms on the right-hand side (from left to right) represent the heat transfer by conduction along the flow direction, the advection in the flow field, the heat transfer by convection between the HTF and the absorber, the side fins, and bottom fin, respectively.

The energy balance describing the insulation on the back side of the collector is expressed as:

$$\begin{aligned} m_{ins}c_{p,ins}\frac{\partial T_{ins}}{\partial t} &= k_{ins}A_{ins}\frac{\partial T_{ins}}{\partial x} \\ &+\frac{k_{har,bfin-ins}\ A_{ins}\left(T_{ins} - T_{bfin}\right)}{\Delta y_{bfin-ins}} \\ &+h_{\infty}A_{ins}(T_{\infty} - T_{ins}). \end{aligned} \quad (17)$$

To solve the system of equations described above for the PV/T collector, the finite difference method is applied with an implicit scheme. The algebraic form of the equation system is solved using MATLAB®.

After the initial development and validation process in MATLAB®, the absorption chiller model and the PV/T collector models are integrated into TRNSYS 18 using the Type 155 component to be able to model the operation of the integrated system model. Type 155 handles the data transfer between the TRNSYS 18 and MATLAB® engine. All other components in the PV/T-driven CCHP system model are selected from the TRNSYS 18 component library. For example, Type 158, Type 138, Type 91, and Type 114 are used to model the hot water storage tank, the auxiliary heater, the heat exchanger, and the pumps, respectively (TRNSYS, 2021).

The space heating and cooling loads of the multi-unit residential building are estimated for the reference year 2011 using EnergyPlus™ and integrated into the TRNSYS model using the Type 682 component. The building's electrical load is not considered in the current study. Details regarding the case study building's geometry, envelope, and orientation can be obtained from a study conducted by Coady and Duquette (2021).

To control the flow rate in the solar collector loop, the state of the incoming solar irradiance is used. The flow rate is activated when the incoming solar irradiance is greater than

150 W/m^2. The charging of the tank is controlled by a differential controller, and this controller activates the flow when the outlet temperature of the PV/T collector array is higher than the temperature of the node located in the lowest part of the storage tank by 8°C. The same controller deactivates the pump when the temperature difference is lower than 3°C. The flow rate in the load (*i.e.*, tank discharging) loop is activated when there is a heating load.

Results

The transient numerical models developed in MATLAB® are verified by comparing simulation outputs with data published in the literature. The verification of the transient absorption chiller model is achieved using scenario data from the numerical study conducted by Ochoa et al. (2016). In the selected scenario, hot water is initially circulated at the generator inlet at a temperature of 75°C and is gradually increased from 75°C to 85°C over a period of 250 s, from which point it remains constant until the end of the simulation. Figure 3 shows a comparison of the numerical and simulation results for the mass flow rate of the strong and weak solutions, and refrigerant vapour over the stated time period. The current predictions fit well with the results from the reference study as the root mean square error (RMSE) between the current predictions and experimental study for the datasets shown is negligible (< 0.002 kg/s).

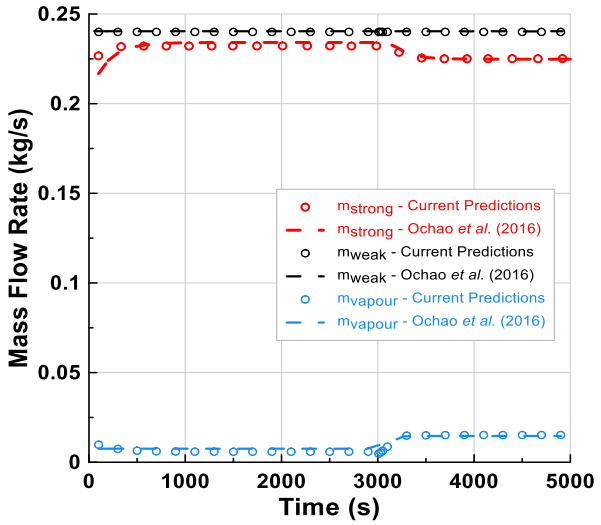

Figure 3. Variation in mass flow rate of strong and weak solutions, and refrigerant vapour for the current study and reference study

To verify the energy balance in the absorption chiller, the average temperature of the external water connections in the generator, absorber, evaporator, and condenser are also compared with those from the reference study. Figure 4 illustrates this comparison and as in the case of the mass balances, a good agreement is found between the current predictions and those from the reference study. The RMSE values corresponding to the external water connection temperature datasets at the absorber, evaporator, condenser, and generator are found to be 0.11°C, 0.35°C, 0.30°C, and 0.49°C, respectively.

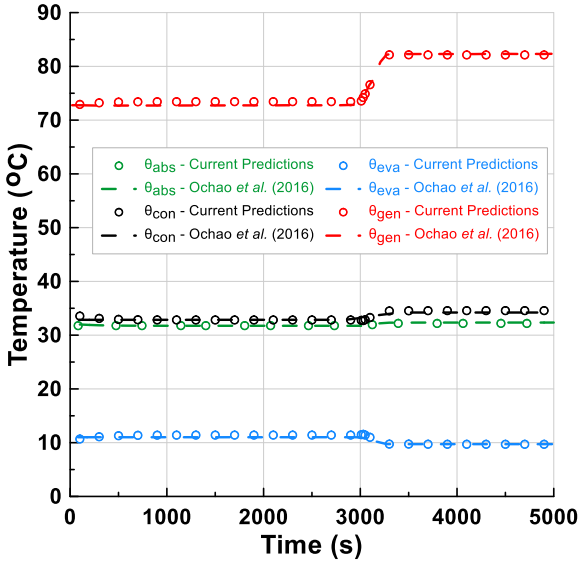

Figure 4. Variation in the average temperature of the external water connections in the generator, absorber, evaporator and condenser for the current study and reference study

The PV/T collector model is validated by comparing predictions from the current study with those from an experimental study conducted by Joshi et al., (2008). The same PV/T collector geometry, and working and boundary conditions are used. The experiment was conducted during the month of May in New Delhi, India. Figures 5 and 6 show the comparison between the simulation and experimental results for the PV/T collector outlet temperature and electrical efficiency, respectively, over a 9 hour period. The simulation results closely match those of the reference study as the RMSE values corresponding to the datasets in the given order are found to be 0.9°C and 0.74%.

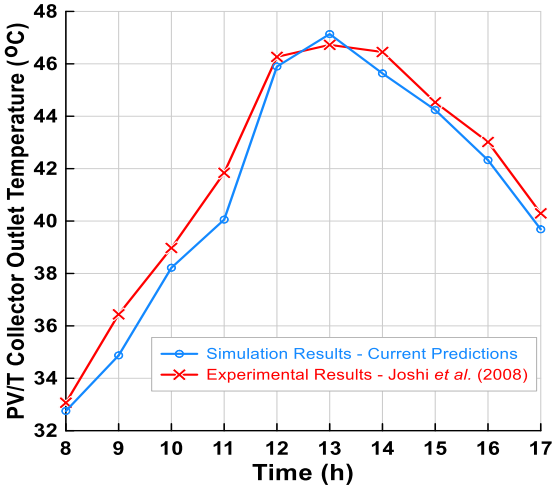

Figure 5. Variation in PV/T collector outlet temperature for the current study and reference study

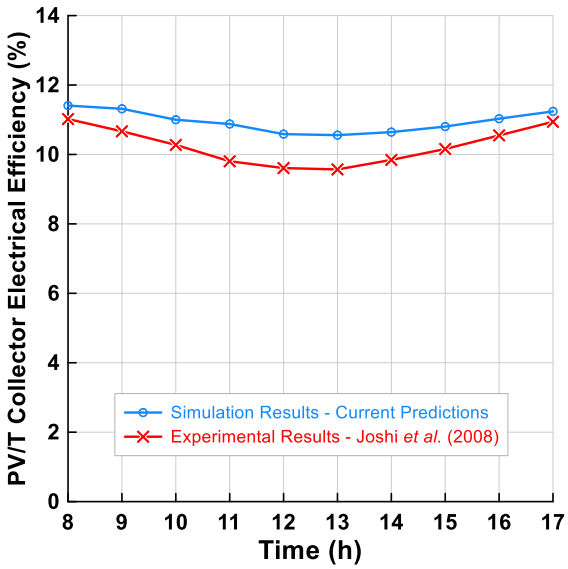

Figure 6. Variation in electrical efficiency of the PV/T collector for the current study and reference study

To verify the integration between the MATLAB® solution algorithm of the absorption chiller and the TRNSYS 18 time loop, the validation case is recreated in TRNSYS 18 using a time dependent forcing function (Type 14). Figure 7 shows that the results are in line with each other, which confirms that there is uniformity between the solution algorithms.

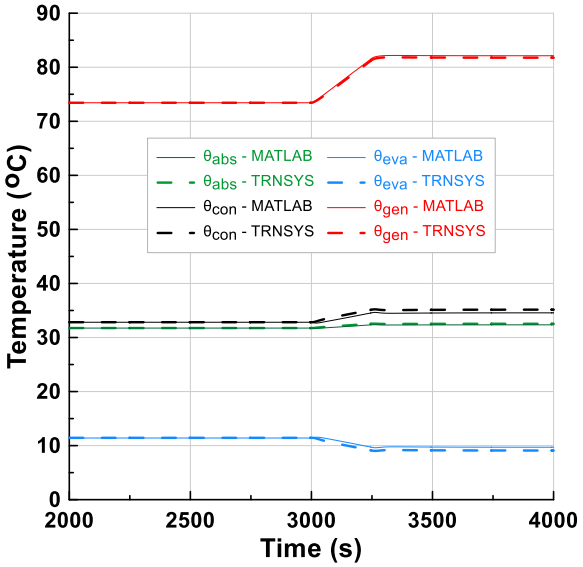

Figure 7. Verification of model operation in MATLAB® and TRNSYS 18

The full PV/T-driven CCHP system model (shown in Figure 1) is simulated over a 24 hour period during the peak heating day (*i.e.*, January 23rd, 2011) of the winter season to assess its performance. Figure 8 shows the PV/T collector array outlet temperature and average water storage tank temperature over the course of the day.

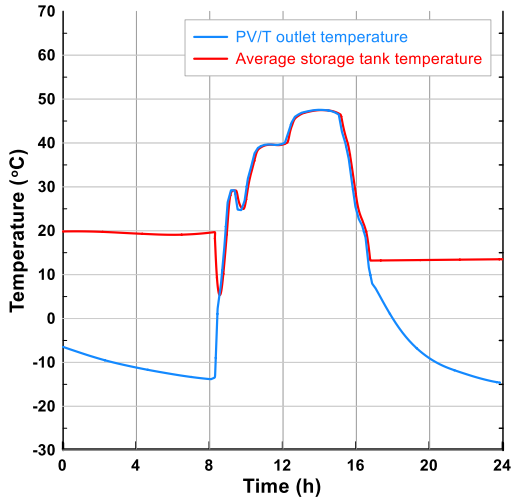

Figure 8. Daily dynamic temperature response of the water storage tank and PV/T collector outlet temperature during the peak winter heating day (January 23rd ,2011)

Due to the low outdoor air temperature experienced throughout the day, the PV/T collector outlet temperature never exceeds roughly 48°C. After sunrise, due to the positive effect of the incoming solar irradiance, the PV/T collectors reach higher temperature levels than the storage tank, which enables solar energy to be utilized for meeting the space heating load. This charging window corresponds to a ~ 6 hour period during the simulated day. Despite the low outdoor air temperature, the PV/T-driven CCHP system is capable of supplying 27.10% of the daily space heating load.

Conclusion

In the current study, transient models representing an absorption chiller and a PV/T collector array have been developed, verified/validated, and integrated within the TRNSYS 18 simulation environment to formulate a PV/T-driven CCHP system model. The system's performance was assessed using estimated space heating load data for a multi-unit residential building located in Ottawa, Canada. It was found that the system is capable of meeting just over one quarter (27.10%) of the building's space heating requirement on the coldest day of the year.

Further analysis is needed to assess how this system performs during the cooling season, as well as performing an analysis from an electrical load standpoint. In the following phase of research, a full-scale building model will be developed in TRNSYS 18 using the multi-zone building component (Type 56). This addition will make it possible to include space conditioning requirements at the zone-level and assess system impacts in-situ.

The current work is the first step toward the development of a fully dynamic PV/T-driven CCHP system model. It will serve as a basis for future model iterations in which the system topology, scale, component sizing, and control strategies will be optimized with the goal of reducing fixed

and operational costs for meeting the energy needs in residential buildings in a variety of climate regions across Canada.

Acknowledgement

This work was supported by the Natural Sciences and Engineering Research Council of Canada (NSERC).

References

Langlois-Bertrand, S., Vaillancourt, K., Beaumier, L., Bahn, O., Mousseau, N. (2021). Canadian Energy Outlook 2021 — Horizon 2060, *Institut de l'énergie Trottier and e3c Hub*, Montreal, Canada.

Sawyer, D., S. Stiebert, R. Gignac, A. Campney, and D. Beugin. (2021). 2020 Expert Assessment of Carbon Pricing Systems. *Canadian Institute for Climate Choices.*

House of Commons, (2018). Better Buildings For a Low-Carbon Future. *Standing Committee on Environment and Sustainable Development.*

Yousefi, H., Ghodusinejad, M.H., Kasaeian, A. (2017). Multi-objective optimal component sizing of a hybrid ICE + PV/T driven CCHP microgrid. *Applied Thermal Engineering*,122.

Kutlu, C., Li, J., Su, Y., Wang, Y., Pei, G., Riffat, S. (2020). Investigation of an innovative PV/T-ORC system using amorphous silicon cells and evacuated flat plate solar collectors. *Energy*,203.

Wang, J.J., Jing, Y.Y., Zhang, C.F. (2010). Optimization of capacity and operation for CCHP system by genetic algorithm. *Applied Energy*,87.

Zeyghami, M., Goswami, D.Y., Stefanakos, E. (2015). A review of solar thermo-mechanical refrigeration and cooling methods. *Renewable and Sustainable Energy Reviews*,51.

Shirazi, A., Taylor, R.A, Morrison, G.L, White, S.D. (2018). Solar-powered absorption chillers: A comprehensive and critical review. *Energy Conversion and Management*,171.

Herrando, M., Pantaleo, A.M, Wang, K., Markides C.N. (2019). Solar combined cooling, heating and power systems based on hybrid PVT, PV or solar-thermal collectors for building applications. *Renewable Energy*,143.

Calise, F., D'Accadia, M.D, Vanoli L. (2012). Design and dynamic simulation of a novel solar trigeneration system based on hybrid photovoltaic/thermal collectors (PVT). *Energy Conversion and Management*,60.

Fong, K.F., Lee, C.K. (2015). Investigation of separate or integrated provision of solar cooling and heating for use in typical low-rise residential building in subtropical Hong Kong. *Renewable Energy*, 75.

Martínez, PJ., Martínez, JC., Martínez, P. (2016). Performance comparison of solar autonomous and assisted absorption systems in Spain. *International Journal of Refrigeration*, 71.

Kohlenbach, P., Ziegler, F. (2008). A dynamic simulation model for transient absorption chiller performance. Part I: The model. *International Journal of Refrigeration*, 31.

Bowie, D., (2016) Experimental Evaluation of a Triple-State Sorption Chiller. Ph.D. Thesis, *Carleton University*.

Tagliafico, L.A., Scarpa, F., de Rosa, M. (2014) Dynamic thermal models and CFD analysis for flat-plate thermal solar collectors - A review. *Renewable and Sustainable Energy Reviews(30)*, 526-537.

Ochoa, A.A.V., Dutra, J.C.C., Henríquez, J.R.G., dos Santos C.A.C. (2016). Dynamic study of a single effect absorption chiller using the pair LiBr/H2O. *Energy Conversion and Management*, 108.

Chow, T. T., He, W., Ji, J. (2006). Hybrid photovoltaic-thermosyphon water heating system for residential application. *Solar energy*, 80(3), 298-306.

Duffie, J. A., Beckman, W. A., Blair, N. (2020). *Solar engineering of thermal processes, photovoltaics and wind.* John Wiley & Sons.

W.C. Swinbank (1963). Long-wave radiation from clear skies, *Quart. J. Roy. Meteorol. Soc. 89* (381), 339–348

Patankar, S. V. (2018). *Numerical heat transfer and fluid flow*. CRC press.

TRNSYS, (2021). TRNSYS 18 - a TRaNsient SYstem Simulation Program – Mathematical Reference.

Coady, J., & Duquette, J. (2021) A techno-economic assessment of residential building energy retrofits in Canada's remote communities: A case study *Proceedings from IBPSA 2021: Canada's eSim.* Vancouver (Canada)